Journal of the European Ceramic Society **18** (1998) 15–22
Published by Elsevier Science Limited
Printed in Great Britain.
PII: S0955-2219(97)00111-8
0955-2219/98/$19.00 + 0.00

Sliding Wear Response of an Alumina–zirconia System

L. Esposito,[a] R. Moreno,[b] A. J. Sànchez Herencia[b] and A. Tucci[a]*

[a]Italian Ceramic Center, Via Martelli 26, 40138 Bologna, Italy
[b]Instituto de Ceramica y Vidrio, SP-28500 Arganda del Rey, Madrid, Spain

(Received 4 March 1997; revised version received 29 April 1997; accepted 30 May 1997)

Abstract

The unlubricated wear behaviour of an alumina–zirconia system was investigated, using a pin-on-disc apparatus, at different sliding speeds. Samples were prepared with different percentages of alumina and zirconia and tested at the same conditions in order to study the influence of the different materials on the wear mechanisms. The morphologies of the worn surfaces and the wear debris were studied using scanning electron microscope (SEM), X-ray spectroscopy (EDX) and X-ray diffraction (XRD) analysis. Different tribological behaviours of the sliding couples were found. For the alumina based ceramics, A (100% Al_2O_3) and AZ (85 vol% Al_2O_3/15 vol% Y–ZrO_2), a critical value of the sliding velocity was found at which a wear transition regime was observed, from plastic deformation to a prevailing fracture mechanism. The tribological behaviour of the zirconia based ceramics, Z (100% TZ–3YS) and ZA (85 vol% Y–ZrO_2/15 vol% Al_2O_3), was influenced considerably by their low thermal shock resistance. Extensive cracking phenomena and high material loss occurred under the testing conditions employed. Published by Elsevier Science Limited.

1 Introduction

There is considerable industrial interest in replacing metallic and polymeric components with structural ceramics due to their chemical inertness, good mechanical characteristics and high resistance to elevated temperatures and thermal shock.

Alumina is a well known material used for low wear components,[1] but its lack of ductility may reduce the field of applications. Zirconia-based ceramics with higher toughness seem to be the candidate materials for tribological applications. Several studies in this regard have provided contradictory results,[2–4] clearly showing as to better understand the wear mechanisms, it is very important to know exactly the geometry of the contact, the working conditions, and the nature of the materials and their characteristics. In such studies there is however unanimous agreement with the fact that under relatively mild conditions, the stress induced by the tetragonal to monoclinic phase transformation of the zirconia improves the wear resistance. However, due to the low thermal conductivity of zirconia, at high sliding speeds the asperity flash temperatures arising from frictional heating and the consequential high stresses generated by thermal shock, cause severe wear.[5–8]

The addition of different percentages of alumina to zirconia results in composites with enhanced fracture toughness with respect to the matrix and with different thermal properties,[9–12] that meaningfully increase their wear resistance

The aim of this investigation was to evaluate and compare the tribological behaviour of zirconia based ceramics and alumina, using a pin-on-disc apparatus at different sliding velocities. Materials with different percentages of alumina and zirconia were prepared and tested at the same conditions to study the different contributions to the wear mechanisms.

2 Experimental procedure

2.1 Sample preparation

An α-Al_2O_3 (Condea HPA05, Germany) and a 3 mol% Y_2O_3 partially stabilised zirconia (TZ–3YS, Tosoh, Japan) were used as starting materials. The main characteristics of these powders are reported in Table 1. The chemical data are from data sheets supplied by the manufacturers. Particle size distributions were determined using a laser Coulter LS130 (USA), specific surface areas by

*To whom correspondence should be addressed.

Table 1. Properties of the powders

Physical–chemical properties	*Al_2O_3 Condea, HPA05*	*Y-TZP Tosoh, TZ–3YS*
Chemical analysis (wt%)		
Al_2O_3	99·99	0·005
ZrO_2	—	95·00
Y_2O_3	—	4·98
SiO_2	0·002	0·002
Na_2O	0·003	0·003
Fe_2O_3	0·001	0·004
Mean particle size (μm)	0·3	0·4
Density (g cm^{-3})	3·88	5·81
Specific surface area (m^2 g^{-1})	9·5	6·7

single point N2 adsorption (Monosorb, Quantachrome, USA) and the density of the powders using a He multipicnometer.

The following four compositions including the two pure compounds and two intermediate mixtures were prepared: A (100% Al_2O_3), Z (100% TZ–3YS), AZ (85 vol% Al_2O_3/15 vol% TZ-3YS) and ZA (85 vol% TZ–3YS/15 vol% Al_2O_3).

Aqueous slips of the different compositions were prepared by mechanically stirring the pure powder or mixture of powders with distilled water at a solid loading of 70wt% and further ball milling with Al_2O_3 balls and jar for 15 h. The deflocculation of the slips was studied from zeta potential and viscosity measurements at different dispersing conditions. The zeta potentials were determined using a mass transport analyser (Micromeritics, USA) on slips containing 20 wt% solids. HCl and NaOH were used for pH adjustments. Rheological studies were carried out using a concentric cylinders viscometer (Haake, Rotovisco RV20, Germany) at 25°C, in which the flow curves are built up by collecting 200 points in both up and down branches while changing the shear rate from 0 to 1000 s^{-1} in 2-min and 1-min dwelling. The flow curves of slips from the two starting powders and the mixtures were measured at different pH conditions.

Once the dispersion behaviour was optimised, slips of the different compositions were cast in plaster of Paris moulds to form plates of 75×75×10 mm and cylinders 5 mm in diameter and 10 mm long. The green casts were dried in air and then presintered at 1100°C for 1 h to facilitate handling. The green densities were measured by the Hg immersion method.

Sintering was carried out at 1550°C for 2 h, and a nearly theoretical density was obtained in all cases. The sintered plates were then machined to obtain discs for the wear experiments and bars for the mechanical tests.

A high purity, high density commercial alumina (Al23 Degussit Germany), AP, was chosen as the pin material. Microstructural observations were made on polished and thermally etched surfaces. The grain size distribution of each phase was determined for each material on scanning electron microscope (SEM) micrographs. The determinations were made assuming that the area enclosed by the closed boundary of a grain is equal to that of a circle. Sintered densities were measured by water immersion. X-ray diffraction analysis was carried out to identify the crystallographic phases.

For the mechanical characterisation the Vickers hardness was measured using a LECO micro-macrohardness apparatus. After testing different loads, the one selected was 196·2N where the ratio c/a was higher than 2·5, except for the pure Al_2O_3 in which an indentation load of 98·1N was used. The K_{Ic} value was calculated according to the equation proposed by Anstis *et al.*[13] Flexural strength was determined by four-point bending on cylindrical cast bars using an universal testing machine (Instron 2511) with 40 and 20-mm outer and inner spans, respectively, and a crosshead displacement rate of 0·5mm min^{-1}. The physical–mechanical characteristics of the materials used as disc and pin materials are reported in Table 2.

2.2 Test parameters

The friction and wear responses of alumina and zirconia-based ceramics were studied using a pin-on-disc apparatus.[14] The discs 40 mm in outer diameter,

Table 2. Characteristics of the ceramic bodies

Characteristics	*Z*	*ZA*	*AZ*	*A*	*AP*
Green density (%)	51·9	55·0	67·4	69·0	—
Sintered density (g cm^{-3})	6·0	5·75	4·27	3·88	3·77
Percentage ZrO_2 tetragonal phase	100	100	100	—	—
Grain size Al_2O_3 (μm)	—	0·75	4·1	4·3	7·3
Grain size ZrO_2 (μm)	0·55	0·56	0·54	—	—
Flexural strength (MPa)	766[a]	—	750[a]	200[a]	215[b]
HV196·2N (GPa)	12·4	13·2	15·7	15·1[c]	15·5
KIC[d] (MPa$\sqrt{m}$)	5·3	4·6	3·2	3·1	4·4

[a]Four-point bending.
[b]Three-point bending
[c]$HV_{98·1N}$.
[d]Anstis *et al.*[13] formula.

14 mm in inner diameter and 8 mm in thickness, were prepared by machining the sintered plates. The features of the unworn surfaces are shown in Fig. 1(a)–(d). The sliding tip of the pins was a hemisphere with a diameter of $5{\cdot}0 \pm 0{\cdot}1$ mm. Before each test, the specimens were carefully cleaned with acetone and their weight was measured using a microbalance (Mettler H14, Switzerland).

Three sliding speeds were chosen, 0·3, 0·7 and $1{\cdot}0\,m\,s^{-1}$, the distance travelled was 3000 m, and the normal applied load was 32·83N. At the end of each test, the weight loss of the discs and pins was measured and the relative volumetric wear rates were calculated. To determine the wear mechanisms and surface degradation processes, the wear scars were examined using a SEM (Jeol T330, Japan), equipped with an energy dispersion X-ray spectroscopy system (EDS).

3 Results

The curves of the zeta potential versus pH, for both $Al2O_3$ and ZrO_2 aqueous slips, show as the isoelectric points occur at pH values of 9 and 7, respectively, thus indicating that in both cases, an acidic medium is required to provide good stability, where the corresponding zeta potentials are high enough to assure the complete stabilisation of the suspended particles.

The rheological behaviour of all the slips, studied at different pH conditions, shows that the minimum viscosity is obtained at pH 4·0 for Al_2O_3 based compositions and at pH 5·1 for ZrO_2 based ones. The intermediate mixtures present a similar behaviour to that of the major phase. The increase in the viscosity observed in this case for lower pH values is probably related to the dissolution of Y^{3+} ions which act as counterions and comprise the double layer.[15] This forming technique allows very dense pure and composite materials to be achieved, with densities close to the theoretical ones. SEM observations of the sintered materials showed a highly homogeneous structure without agglomerates and abnormally grown alumina grains. There are very few defects and the grains are prevalently submicrometric with a narrow grain size distribution.

In Fig. 2, the average values of the coefficient of friction measured for the different sliding pairs are

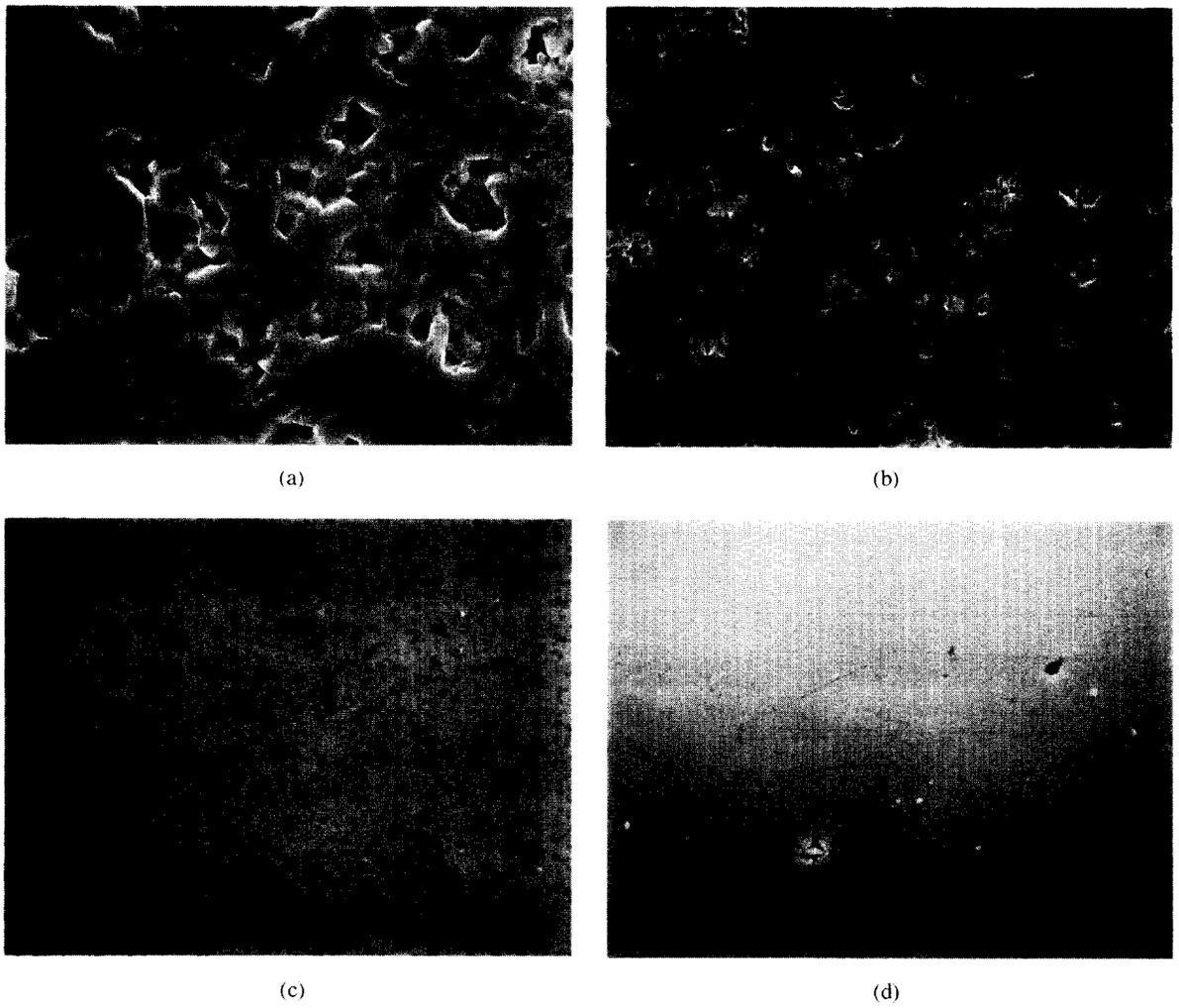

(a) (b) (c) (d)

Fig. 1. SEM micrograph of the unworn surface (a) of the disc A, (b) of the disc AZ, (c) of the disc ZA and (d) of the disc Z.

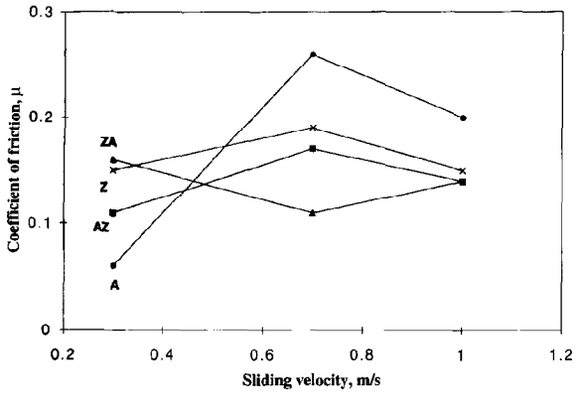

Fig. 2. Coefficient of friction, μ, of the tested couples as a function of sliding velocity.

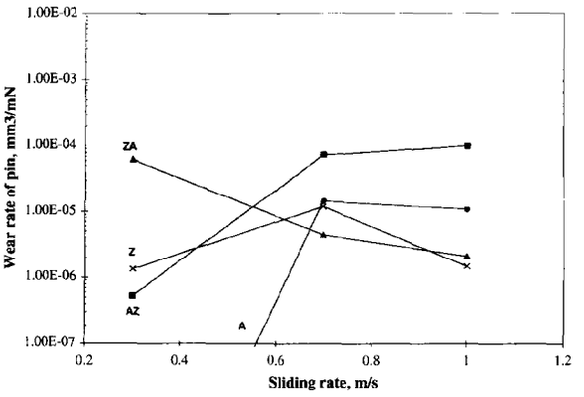

Fig. 4. Wear rates of the pins as a function of sliding velocity, in a semi-logarithmic diagram.

reported as a function of the sliding velocity. For the couples with zirconia based ceramics there is not a significant variation in the average μ values at the different sliding conditions, a meaningful increase in the coefficient of friction is shown over $0{\cdot}3\,m\,s^{-1}$ for the A–AP pairs, from 0·06 at $0{\cdot}7\,m\,s^{-1}$ it reaches 0·26 at $0{\cdot}7\,m\,s^{-1}$.

Figures 3 and 4 report the wear rates as a function of sliding velocity for the discs and pins, respectively; a semilogarithmic scale is used.

For the two alumina based ceramics, A and AZ, at $0{\cdot}3\,m\,s^{-1}$, both the discs and pins show the lowest wear rate, less than $10^{-6}\,mm^3\,(mN)^{-1}$, and the pin slid against the alumina disc does not show any detectable weight loss.

The worn surfaces of the discs of both materials appear polished and smoother than the original ones (Fig. 5). At higher magnification, many small cylindrical particles, of about 0·1 μm in diameter and 0·5–10·0 μm in length can be seen on the surface of the wear track of the disc A (Fig. 6). The rolled shaped debris, as detected by the EDS system, contains only aluminium, they might be aluminium hydroxides, as suggested in other studies.[16–18] The very low coefficient of friction found for the A–AP couples, also in comparison with the AZ–AP couple, is to be associated with the presence of these particles. On the worn surface of the corresponding pins the very small area where the contact was created, is perfectly polished.

At a higher sliding velocity $0{\cdot}7\,m\,s^{-1}$ and $1{\cdot}0\,m\,s^{-1}$, there is a meaningful increase in the wear rate of the A and AZ discs, of almost two orders of magnitude. The wear tracks of the A discs are characterised by a general fracture of the alumina grains and accumulation and compaction of the wear debris in a thin surface layer, adhering both to the disc and pin surfaces (Fig. 7).

The AZ worn surface is characterised by a more smooth surface, due to the high grade of plasticization of the compacted debris (Fig. 8), supported by the presence of the zirconia.

Increasing the content of zirconia in the disc material clearly causes more wear at the same testing conditions. The wear rate found for the ZA discs is not affected by the different sliding velocities. For the Z discs, the wear rate increases slightly from $0{\cdot}3\,m\,s^{-1}$ to $0{\cdot}7\,m\,s^{-1}$, while at

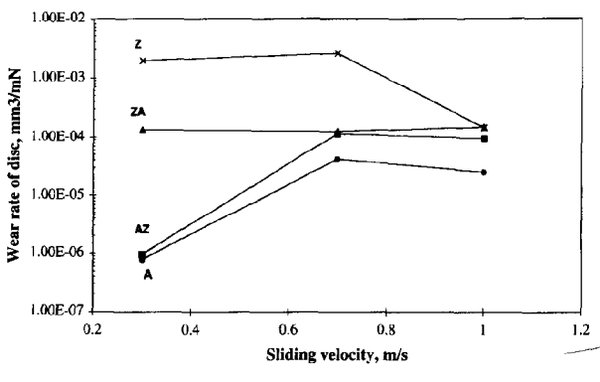

Fig. 3. Wear rates of the discs as a function of sliding velocity, in a semi-logarithmic diagram.

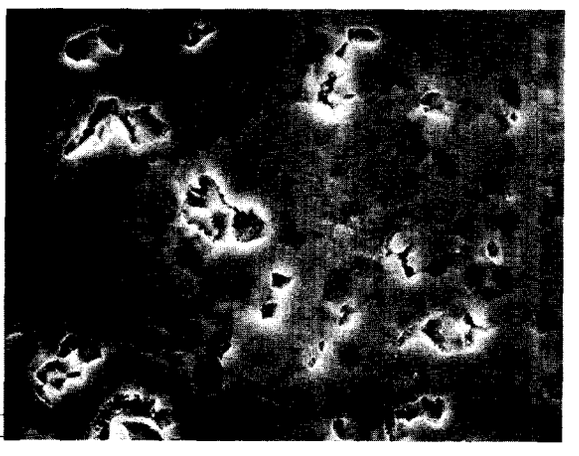

Fig. 5. SEM micrograph of the worn surface of the disc A, after the test at $0{\cdot}3\,m\,s^{-1}$.

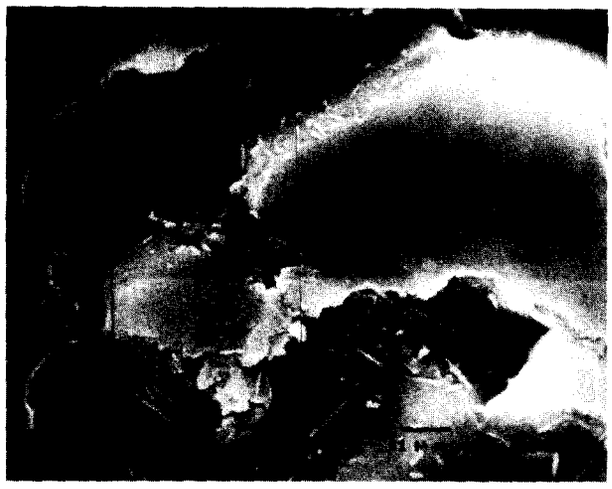

Fig. 6. Magnification of Fig. 5, showing the presence of cylindrical debris.

Fig. 8. SEM micrograph of the worn surface of the disc AZ, after the test at $0{\cdot}7\,m\,s^{-1}$.

$1{\cdot}0\,m\,s^{-1}$, it abruptly decreases reaching the same value of the ZA disc. The morphology of the wear track of the discs in ZA and Z is rather similar, with large smooth areas of plastically deformed material, oriented in the sliding direction, near rougher areas where the surface layers have been removed by chipping due to extensive fractures (Fig. 9). The worn surfaces of the corresponding pins are characterised by the presence of strongly adhering large lamina of material detached from the disc (Fig. 10).

As the sliding velocity increases, little change occurs in the features of the worn surfaces of the disc; they are always characterised by extended fractures and adhesion phenomena of disc material on the pin surface.

For the ZA–AP and Z–AP couples, the X-ray diffraction analyses conducted on the wear debris collected after the tests, when sufficient amounts were available, showed no notable tetragonal-to-monoclinic phase transformation for the zirconia material.

4 Discussion

Comparison of the tribological responses of the ceramics with different alumina and zirconia contents, shows that the wear is affected considerably by the test conditions, in this case by the sliding velocity, and the wear mechanisms involved are influenced by the nature of the materials coupled.

For the A–AP couple, $0{\cdot}3\,m\,s^{-1}$ represents a test condition of mild wear. The counterfaces are only slightly polished by nonindenting asperities of the harder pin material, i.e. a sort of 'soft abrasion' mechanism takes place without generating fractures. Furthermore, under this condition the formation of cylindrical debris on the counterfaces of the coupled materials is related, according to other authors,[16,17] to the formation of a thin aluminium hydroxide film. Such a tribochemical film has a layered structure and is softer than the alumina substrate.[19] It is easily destroyed during the sliding and rolled to form cylindrical debris. These debris

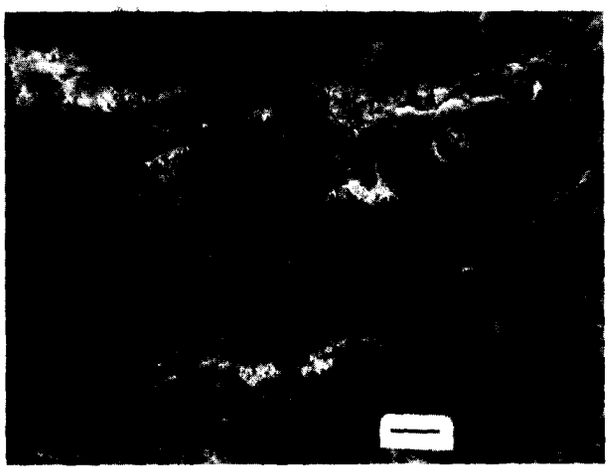

Fig. 7. SEM micrograph of the worn surface of the disc A, after the test at $0{\cdot}7\,m\,s^{-1}$. The bar is $13\,\mu m$ long.

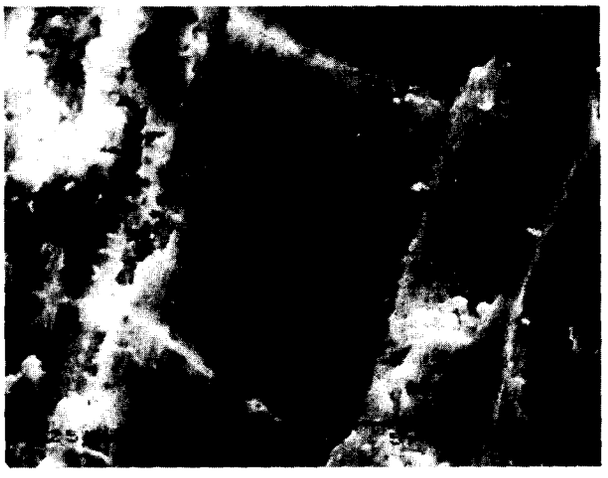

Fig. 9. SEM micrograph of the worn surface of the disc ZA, after the test at $1{\cdot}0\,m\,s^{-1}$. Long straight cracks are visible.

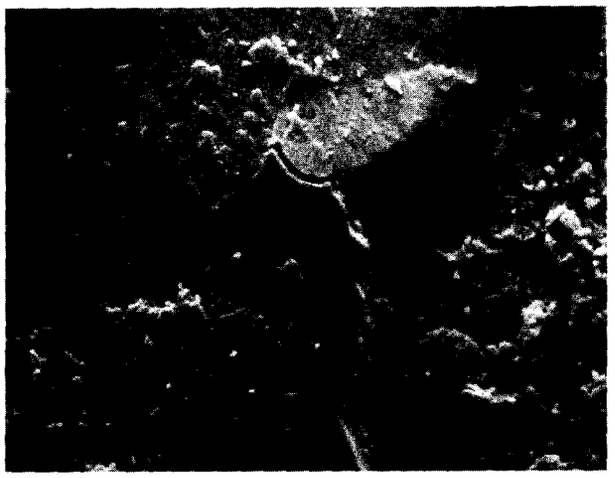

Fig. 10. SEM micrograph of the surface of the pin AP, slid against the ZA material after the test at $1{\cdot}0\,m\,s^{-1}$. Large lamina of the disc material are visible.

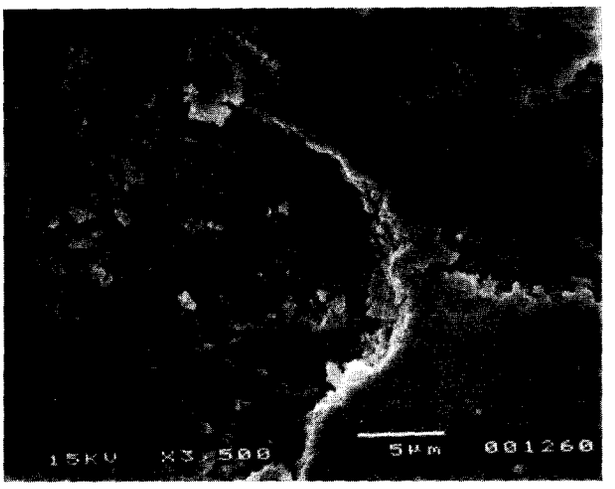

Fig. 11. SEM micrograph of the worn surface of the disc Z, after the test at $1{\cdot}0\,m\,s^{-1}$.

may act as roller bearings, explaining the reduced friction and wear found for this couple.

At higher sliding velocities, both friction and wear increase. The wear mechanisms involved are mainly due to surface fracture, intergranular for the coarser grained alumina of the pin and transgranular for the finer disc material, with the production of a large amount of debris. In the pin-on-disc geometry, tensile stress is generated behind the sliding contact pin. When it reaches a threshold value, cracks can arise inside the material. These cracks propagate during sliding until the detachment of a grain or fragment of grains occurs. In this condition the coefficient of friction abruptly increases as a result of both the higher roughness of the coupled surface and the injection of large debris at the interface.

For the Z–AP couple, the friction and wear behaviours are affected considerably by the interfacial temperatures and difference in hardness between the coupled materials. The alumina pin, harder than the zirconia, at the beginning of the test acts as an indenter on the softer disc material, the debris so formed are crushed by the compressive forces present, compacted and slightly deformed in very smooth layers (Fig. 11). The debris formed in this way adhere to the counterfaces, progressively changing the Z–AP contact into a new Z–Z contact. Furthermore, due to the very low thermal diffusivity of the Z material,[19–23] the flash temperatures and the microscopic temperature pulses arising from point contact, can reach elevated values and large thermal gradients located in small areas are created. At this point, thermal shock stresses become relevant, explaining the extensive fracture observed. During sliding, these cracks propagate until detachment of layers of disc material occurs (Fig. 12), contributing to a severe increase in wear. At the highest sliding velocity, $1{\cdot}0\,m\,s^{-1}$, the effect of the thermal shock on the disc material is lower than at 0·3 and $0{\cdot}7\,m\,s^{-1}$, and the disc wears less. The very high flash temperature arising at the microcontacts reduces the driving forces for the stress induced tetragonal to monoclinic phase transformation, explaining the lack of monoclinic zirconia in the XRD patterns of the debris.

The same mechanisms are active in the ZA–AP couple. Also in this case, ZA material is subjected to plastic deformation and thermal shock induced fracture. But, because the addition of 15% of alumina to the Y–TZP causes an increase in hardness and thermal shock resistance,[22] the wear rate is significantly lower and in practice unaffected by the sliding speed.

The wear mechanisms for the couple AZ–AP are more similar to those of the A–AP couple. The sliding speed $0{\cdot}7\,m\,s^{-1}$ represents the condition for which there is a transition from a plastic

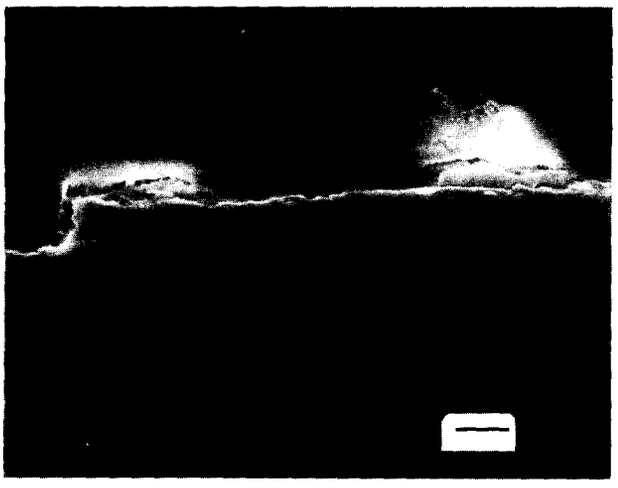

Fig. 12. SEM micrograph of the cross section of the worn surface of the disc Z, after the test at $0{\cdot}7\,m\,s^{-1}$. The bar is 5 μm long.

deformation to brittle fracture dominated wear process. Although the wear rate of AZ at 0·7 and 1·0 m s^{-1} is rather similar to that of ZA, the wear mechanisms are different. For the AZ material the effect of thermal shock induced brittle fracture seems to be rather low, in fact no long cracks are observed on the wear scars. The loss of material proceeds through the fracture of grains, both intragranular and transgranular (Fig. 13).

Regarding the wear rate of the pins (Fig. 4), it is possible to recognise two different trends. The pins coupled with A and AZ show a significant increase in wear as the sliding velocity increases. For the pins tested against ZA and Z materials, the wear decreases or remains almost constant with increasing sliding velocity. In the first case 0·7 m s^{-1} also represents a transition point for the alumina pin from mild to severe wear, characterised by subsurface brittle cracks (Fig. 14), in the second, the adhesion of thicker sheets of compacted and strongly deformed debris on the pin surface limits its wear (Fig. 10) and also causes an anomalous weight variation at the end of the tests.

Fig. 13. SEM micrograph of the worn surface of the disc AZ, after the test at 0·7 m s^{-1}.

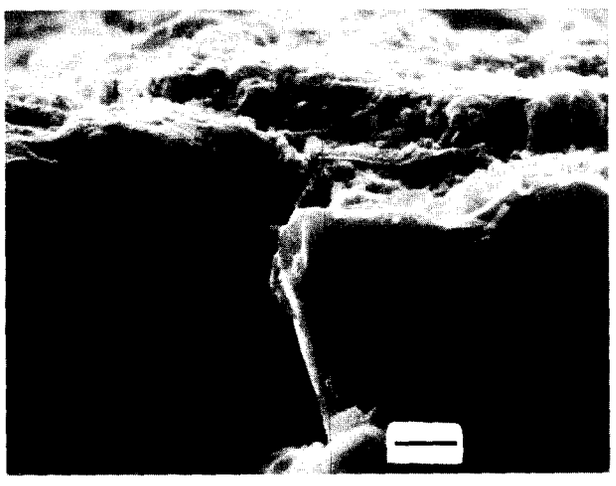

Fig. 14. SEM micrograph of the cross section of the worn surface of the pin AP, slid against the AZ disc, after the test at 0·3 m s^{-1}. The bar is 1·3 μm long.

5 Conclusions

The tribological response of an alumina–zirconia system including the pure materials and two intermediate mixtures prepared via slip casting and denoted as A (100% Al_2O_3), Z (100% TZ–3YS), AZ (85 vol% Al_2O_3/15 vol% TZ–3YS) and ZA (85 vol% TZ–3YS/15 vol% Al_2O_3), was investigated using a pin-on-disc apparatus with the pin constructed from the same high purity high density commercial alumina, AP. Use of the same testing conditions made it possible to study the influence of the disc composition and microstructure on the wear mechanisms. The results obtained can be summarised as follows:

- For the A and AZ materials, a critical value of the sliding velocity was found at which a wear transition regime was observed, from plastic deformation to a prevailing fracture mechanism.
- The wear behaviour of the Z and ZA materials is influenced considerably by the low thermal shock resistance of zirconia. Consequently, extensive cracking phenomena and high material loss were recorded.
- The zirconia content in the ZA and AZ materials produces different wear mechanisms, even though at the highest sliding speed, 1·0 m s^{-1}, the wear rate is approximately the same.

References

1. Jahanmir, S., Tribological applications for advanced ceramics. *Mater. Res. Soc. Symp. Proc.*, 1989, **140**, 285–291.
2. Fischer, T. E., Anderson, M. P. and Jahanmir, S., Influence of fracture toughness on the wear resistance of yttria-doped zirconium oxide. *J. Am. Ceram. Soc.*, 1989, **72**, 252–257.
3. Reuhkala, P. J., Lepisto, T. T. and Måntilå, T. A., Stability and sliding wear behaviour of TZP ceramics in immersed solutions. *Ceramica Acta*, 1991, **3**, 37–44.
4. Woydt, M., Kadoorit, J., Habig, K. H. and Hausner, H., Unlubricated sliding behaviour of various zirconia-based ceramics. *Journal of the European Ceramic Society*, 1991, **7**, 135–145.
5. Asif, S. A. S., Muthu, D. V. S., Sood, A. K. and Biswas, S. K., Surface damage of yttria–tetragonal zirconia polycrystals and magnesia-partially-stabilised zirconia in single-point abrasion. *J. Am. Ceram. Soc.*, 1995, **78**, 3357–3362.
6. Aronov, V., Friction induced straightening mechanisms of magnesia partially stabilised zirconia. *ASME, J. Tribol.*, 1987, **109**, 531–536.
7. Tucci, A. and Esposito, L., Microstructure and tribological properties of ZrO_2 ceramics. *Wear*, 1994, **172**, 111–119.

8. Erdemir, A., A review of the lubrication of ceramics with thin solid films. In *Friction and Wear of Ceramics*, ed. S. Jahanmir. Marcel Dekker, New York, 1994, pp. 119–162.
9. Wang, D., Li, J. and Mao, Z., Study of abrasive wear resistance of transformation toughened ceramics. *Wear*, 1993, **165**, 159–167.
10. He, C., Wang, Y. S., Wallance, J. S. and Hsu, S. M., Effect of microstructure on the wear transition of zirconia-toughened alumina. *Wear*, 1993, **162–164**, 314–321.
11. Lutz, E. H., Swain, M. V. and Claussen, N., Thermal shock behaviour of duplex ceramics. *J. Am. Ceram. Soc.*, 1991, **74**, 19–24.
12. Trabelsi, R., Treheux, D., Orange, G., Fantozzi, G., Homerin, P. and Thevenot, F., Relationship between mechanical properties and wear resistance of alumina–zirconia ceramic composites. *Tribol. Trans.*, 1989, **32**(1), 77–84.
13. Anstis, G. R., Chantikul, P., Lawn, B. R. and Marshall, D. B., A critical evaluation of indentation techniques for measuring fracture toughness: I. Direct crack measurements. *J. Am. Ceram. Soc.*, 1981, **64**(9), 533–538.
14. Esposito, L., Tucci, A., Solomah, A. G. and Palmonari, C., Effects of temperature and sliding velocity on dry tribological characteristics of high purity, high density polycrystalline aluminium oxides. *Wear*, 1992, **153**, 351–360.
15. Fariñas, J. C., Moreno, R., Requena, J. and Moya, J. S., Acid-basic stability of Y-TZP ceramics. *Mat. Sci. Eng.*, 1989, **A109**, 97–99.
16. Block, P., Platon, F. and Kapleski, G., Tribological and interfacial phenomena in Al_2O_3/SiC couples at high temperature. *Journal of the European Ceramic Society*, 1988, **5**, 151–164.
17. Jahanmir, S. and Dong, X., Wear mechanisms of aluminum oxide ceramics. In *Friction and Wear of Ceramics*, ed. S. Jahanmir. Marcel Dekker, New York, 1994, pp. 15–49.
18. Esposito, L. and Tucci, A., Microstructural dependence of friction and wear behaviour in low purity alumina ceramics. *Wear*, in press.
19. Gates, R. S., Hsu, S. M. and Klaus, E. E., Tribochemical mechanism of alumina with water. *Tribol. Trans.*, 1989, **32**, 357–363.
20. Lee, S. W., Hsu, S. M. and Shen, M. C., Ceramic wear maps: zirconia. *J. Am. Ceram. Soc.*, 1993, **76**, 1937–1947.
21. Ishitsuka, M., Sato, T., Endo, T., Shimada, M. and Arashi, H., Raman microprobe spectroscopic studies on thermal shock fracture of ZrO_2-based ceramics. *J. Mater. Sci. Letters*, 1989, **8**, 638–640.
22. Ishitsuka, M., Sato, T., Endo, T. and Shimada, M., Thermal shock fracture behaviour of ZrO_2-based ceramics. *J. Mater. Sci. Letters*, 1989, **24**, 4057–4061.
23. Ishitsuka, M., Sato, T., Endo, T. and Shimada, M., Grain size dependence of thermal shock resistance of yttria-doped tetragonal zirconia. *J. Am. Ceram. Soc.*, 1990, **73**, 2523–2525.